Interfacial Structure of Photoresist Thin Films in Developer Solutions[#]

Vivek M. Prabhu *, Bryan D. Vogt, Wen-li Wu, Jack F. Douglas, Eric K. Lin, Sushil K. Satija [†], Dario L. Goldfarb [‡], Hiroshi Ito [§]

Polymers Division, † Center for Neutron Research, National Institute of Standards and Technology, Gaithersburg, MD 20899; ‡ IBM T. J. Watson Research Center, Yorktown Heights, NY 10598; § IBM Almaden Research Center, San Jose, CA 95120

ABSTRACT

A depth profile of the base developer counterion concentration within thin photoresist films was measured *in-situ* using contrast variant specular neutron reflectivity to characterize the initial swelling stage of the film dissolution. We find a substantial counterion depletion near the substrate and an enrichment near the periphery of the film extending into the solution. These observations challenge our understanding of the charge distribution in photoresist and polyelectrolyte films and are important for understanding film dissolution in medical and technological applications.

Keywords: resist swelling, developer, dissolution, LER, reflectivity

1. INTRODUCTION

The transformation of a solid-like film into a solution upon exposure to a miscible solvent is a complex process involving kinetic pathways associated with the slow transport of the liquid into the film and the evolution of the thermodynamic driving forces during the course of the dissolution process. In complex materials such as polymers, this process occurs in stages from the transformation of the glassy or crystalline film into a swollen gel-like state, followed at much longer times by the final dissolution of the film [1,2]. Recent advances in measurement have allowed a better characterization of this technologically important process. Hinsberg et al. have summarized distinct experimentally observable dissolution and swelling behaviors [1,3] using a tandem quartz crystal microbalance and visible reflectometry setup. These observations are tabulated for a variety of photoresist materials and are qualitatively predicted and understood using a stochastic kinetics simulation [4,5]. All the resists studied would be classified as polyelectrolytes, as they should ionize in the aqueous base developers.

In this paper, the initial stage of polyelectrolyte dissolution is probed by measuring the base counterion distribution within an ultrathin film (360 Å) that ionizes and swells in response to an aqueous base solution. Under the experimental conditions that we consider, the dissolution rate is greatly reduced, thus enabling a measurement of the counterion distribution during the initial stages of the dissolution process; corresponding to one specific case from Hinsberg's observations.

*vprabhu@nist.gov

Advances in Resist Technology and Processing XXII, edited by John L. Sturtevant, Proceedings of SPIE Vol. 5753 (SPIE, Bellingham, WA, 2005)
0277-786X/05/$15 · doi: 10.1117/12.598956

Specular neutron reflectivity (NR) with selectively deuterium labeled base counterions is utilized to measure the counterion distribution within this (weak polyelectrolyte) film. A zero-average contrast (ZAC) NR technique matches the scattering length density (SLD) of the solvent to the thin solid polymer film, rendering the film nearly indistinguishable from the solvent. Introducing small quantities of deuterium-labeled base into the equilibrating solution results in negligible changes in the average solution SLD, but the base is observed by its accumulation within the film. To complement these measurements, a full contrast (FC) method, where the solvent is pure D_2O, is used to measure the polymer profile.

2. EXPERIMENTAL

Poly(norbornene hexafluoroisopropanol) (PNBHFA) ($M_{r,w}$ = 25,000, $M_{r,w}/M_{r,n}$ = 2.27) was spin coated from propylene glycol methyl ether acetate onto silicon wafers primed with hexamethyldisilazane (HMDS) vapor. Unfortunately, the exo / endo isomer content was not determined for the current batch of PNBHFA. As the present study progressed, the importance of the isomer effect was reported [6]. Neutron reflectivity was performed on the NG 7 reflectometer at the NIST Center for Neutron Research. The neutron beam entered through the 12.7 mm thick silicon wafer substrate, reflected from the polymer-liquid interface and was detected at the specular condition as a function of angle (θ) in absolute reflected intensities (R). Measurements were performed as a function of scattering wave vector (Q) normal to the film, $Q = 4\pi\lambda^{-1} \sin\theta$, where λ is the fixed incident neutron wavelength of 4.75 Å with resolution $\Delta\lambda/\lambda = 0.025$. The reflectivity data are modeled with a Parratt algorithm to determine the elastic coherent neutron scattering length density ($Q_C^2 = 16\,\pi\,\rho$) profile, where ρ is the scattering length density. Uncertainties are calculated as the estimated standard deviation from the mean. In the case where the limits are smaller than the plotted symbols, the limits are left out for clarity. For the ZAC–NR experiment, a D_2O / H_2O mixture containing 0.376 volume fraction D_2O, which matches the dry polymer film Q_C^2 of 1.03×10^{-4} Å^{-2}, was equilibrated against the polymer film using a liquid cell with and without added deuterium labeled d_{12}-tetramethylammonium (*d*-TMA) hydroxide (Cambridge Isotopes*). This base counterion was chosen for convenience of a high Q_C^2, rather than the protonated material. Full contrast experiments used protonated TMAH in D_2O to maximize the contrast between polymer and solvent.

Quartz crystal microbalance (QCM) measurements (Q-Sense) were performed by spin coating solutions upon 5.0 MHz AT-cut quartz resonators with silica coated gold electrodes. The quartz resonant frequency change was monitored as a function of time upon equilibration first with pure water and then dilute aqueous base developer solutions using a liquid cell and a peristaltic pump at a rate of 1.0 cm^3/min. Interpretation of film thickness was performed using the Sauerbrey equation.

---

* Certain equipment, instruments or materials are identified in this paper in order to adequately specify the experimental details. Such identification does not imply recommendation by the National Institute of Standards and Technology nor does it imply the materials are necessarily the best available for the purpose.

Selected samples were measured using a Digital Dimension 3000 atomic force microscope (AFM) in tapping mode. The acquired images were corrected with a plane-fit and the root-mean square roughness obtained using the AFM software.

3. RESULTS AND DISCUSSION

3.1.Quartz Crystal Microbalance Swelling Experiments

It is well known that in 0.26 N TMAH developer this PNBHFA has rapid swelling upon contact with developer, followed by dissolution as shown in Figure 1a. This particular dataset was taken using an instrument described elsewhere [3]. Upon diluting the developer strength a stable film swelling behavior is observed, as shown in Figure 1b using the Q-sense instrument. This swelling reaches equilibrium on timescales appropriate for further studies by neutron reflectivity. A transition between swelling to dissolution occurs between (0.10 and 0.18) M.

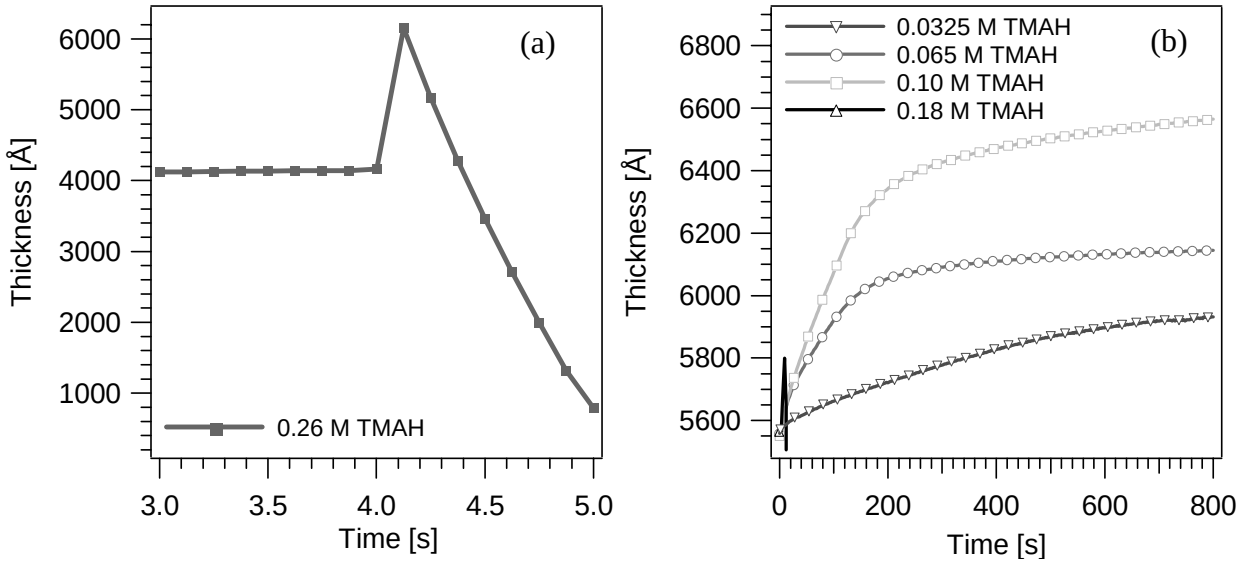

Figure 1. (a) PNBHFA in standard developer 0.26 N TMAH exhibiting rapid swelling and dissolution. (b) Influence of reduced developer strength.

3.2.Neutron Reflectivity – Zero Average Contrast

Figure 2 shows the Fresnel-reflectivity normalized plots for ultrathin films equilibrated at different base concentrations. A very low level of reflectivity (inset), $O(10^{-5})$ beyond Q = 0.02 Å^{-1}, was observed for the film equilibrated with the pure ZAC solvent, indicating an excellent contrast match. The reflectivity is enhanced when base was introduced to the solvent for 0.00074 M (pH = 10.1), 0.010 M , 0.0325 M and 0.065 M *d*-TMA concentrations. The shift in the fringe maxima to lower Q indicates film swelling with increased base concentration. The enhanced amplitude of reflectivity corresponds to an increased contrast between the film and solvent arising from the penetration and condensation of *d*-TMA counterions within the film.

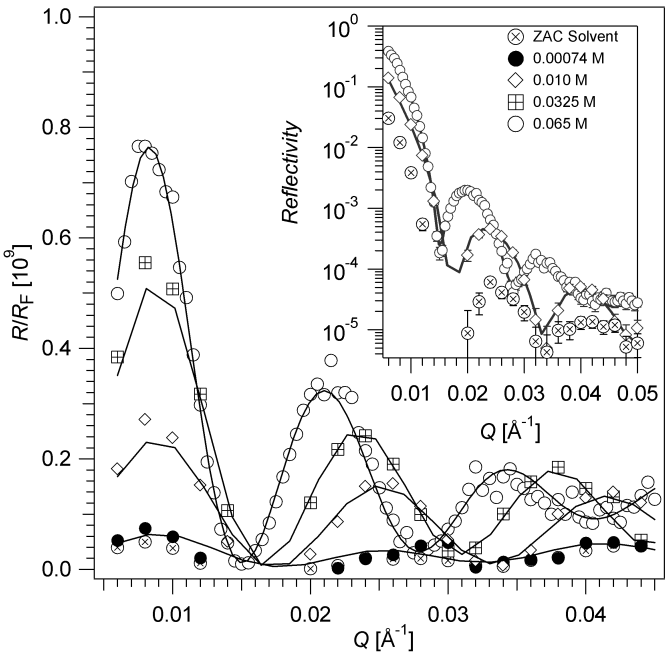

Figure 2. Enhanced Fresnel-normalized reflectivity (R/R_F) upon equilibration with increased concentrations of *d*-TMAH using ZAC solvents. Inset contains the absolute reflected intensities.

The ionization of the chains induced by the base concentration increase leads to the formation of a long-lived gel-like layer before the final dissolution process. The resultant $Q_C^2(z)$ profiles from the fits to the reflectivity data are direct measures of the *d*-TMA counterion concentration associated with the initial stages of photoresist dissolution. The *d*-TMA volume fraction, $\phi_{d\text{-}TMA}$, was calculated from

$$\phi_{d-TMA}(z) = \frac{Q_{C,p}^2 - Q_{C,film}^2(z)}{Q_{C,p}^2 - Q_{C,d-TMA}^2} \quad , \qquad (1)$$

which is valid for a ZAC solvent. $Q_C^2{}_p$ and $Q_C^2{}_{film}$ correspond to the dry and wet polymer film, respectively. The $\phi_{d\text{-}TMA}(z)$ depth profiles, presented in Figure 3, show the extent of film swelling as well as non-uniform base distribution at both the substrate / polymer and the polymer / liquid interfaces. Similar data were shown for strong polyelectrolyte brushes [7] in which ionization is present under neutral pH conditions. However, in these experiments, a pH greater than the acid dissociation constant (pK_a) results in increased chain segmental ionization (due to the chemical equilibrium) and decreases the Debye screening length (κ^{-1}), leading to enhanced electrostatic screening. At high degrees of ionization, the chain conformation expands from the initial dimensions, due to charge-charge repulsion between monomer segments and increased osmotic mixing pressure from the dissociated ions within the film, as found with neutralized polyelectrolyte gels [8]. At the lowest base concentration (0.00074 M), the long-ranged electrostatic interactions are significant (κ^{-1} = 96Å), while the screening length decreases to 12 Å at 0.065 M. Hence, the role of the ionic osmotic pressure, quantified by the base counterion concentration within the film, appears

to be a dominant contribution to these initial stages of dissolution due to the reduced screening length.

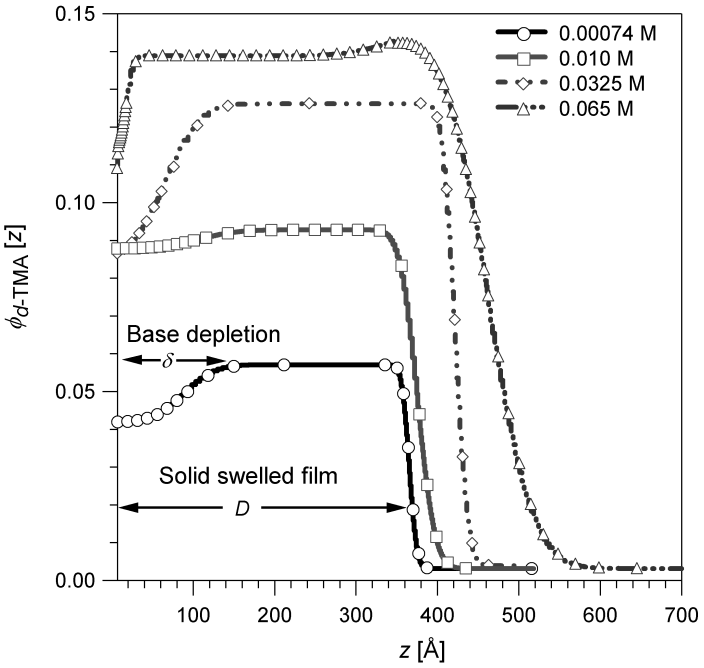

Figure 3. *d*-TMA counterion profiles within polyelectrolyte films versus distance from the silicon substrate with depleted level at the substrate and interfacial broadening at the solid / liquid interface.

3.2.1. Polymer Segmental Ionization

The average polymer segmental degree of ionization (Θ) was estimated as the ratio of the number of base molecules to PNBHFA segments,

$$\Theta = \frac{n_{TMA^+}}{n_{PNBHFA}} = \frac{\phi_{TMA}}{\phi_{PNBHFA}} \frac{\nu_{PNBHFA}}{\nu_{TMA}}, \qquad (2)$$

assuming each base titrates a hexafluoroisopropanol (HFA) proton; ν is the partial molar volume for the respective component and ϕ_{PNBHFA} is determined by the ratio of dry to swollen film (D_0 / D). This is the swelling extent as discussed by Flory[9]. The degree of ionization is well below 100 % within the film, as shown in Figure 4a, reaching a plateau at 47 % for 0.065 M; a lower bound for Θ before dissolution [10] that occurs spontaneously with exposure to higher base concentration. The average ionization fraction is currently an assumed quantity in polymer photoresist material dissolution models, but many variables can affect its value [11]. Figure 4b shows the linear dependence of the film expansion extent (D / D_0) versus Θ. This dependence cannot be described by either dilute solution approximations for equilibrium polyelectrolyte gels [8], nor a uniform chain expansion of a concentrated polyelectrolyte solution at low ionic strength [12]. While the swollen film can be considered a concentrated solution, a dielectric mismatch at the polymer / substrate interface may be essential to understand this apparent linear dependence. At the highest base concentration

examined, 47 % of the chain segments are ionized, yet dissolution does not proceed due to the gelation.

Stable gels in polymer networks arise from interchain interactions due to topological effects and direct chain-chain and chain-surface associations, as well as physical cross-links. Here, the extended hydrogen bonding and hydrophobic nature of the fluorine-containing HFA moieties are the predominant interactions. Observation of a fast swelling and multi-stage dissolution [1] is common. After these initial stages of dissolution, the intermediate stage involves the cascading release of chains and a redistribution of the base counterion species. This evolving counterion structure as the base is transported throughout the film is made via accessible HFA groups. The dry PNBHFA films contain (23 to 30) % free HFA groups that are not associated by hydrogen bonding [13]. A measure of the kinetics of counterion penetration is the next challenge, given our results for describing the interfacial structure is the initial stage of this process.

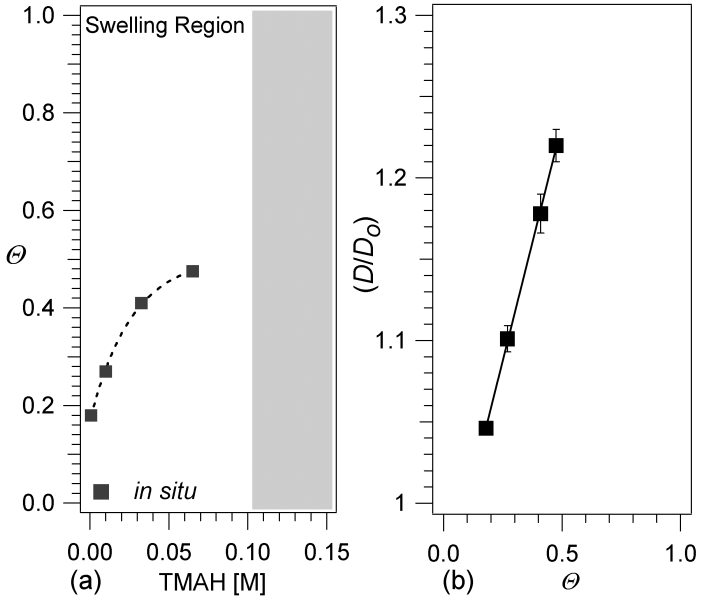

Figure 4. (a) Degree of polymer segment ionization (Θ) versus base concentration illustrating the lower limit of weak polyelectrolyte ionization before dissolution occurring above 0.10 M. (b) Expansion extent dependence on the calculated degree of ionization.

3.2.2. Influence of Solid Substrate

The base depletion near the substrate and a broadening of the free interface of the film are unanticipated effects. The substrate / polymer interface shows a persistent depletion of base with a decreasing depletion range (δ) at higher base concentration as shown in Figure 3. The surface interfacial interaction provided by the adhesion promoter HMDS supports a hydrophobic interface (water contact angles of 72 ± 1°), however accessible Si-OH groups can ionize under these experimental conditions. Although non-equilibrium swelling would account for this non-uniformity, the NR measurements were initiated after a saturation of the swelling, as confirmed by quartz crystal microbalance experiments shown in Figure 1b. The lowest *d*-TMA concentration with a pH = 10.1,

greater than the pKa of HFA [13], show a bulk uptake of $\phi_{d\text{- TMA}}$ = 0.057, yet a depletion to 0.042 occurs over the first 130 Å. Similarly, there is a depletion in the base concentration over the first 140 -145 Å from the substrate for 0.01 M and 0.0325 M solutions. In the case of 0.01 M solution, the experiment reused the same sample from pH = 10.1 leading to a reduced depletion extent. This change in protocol led to an irreversible condensation of base within the film. Fresh samples were used throughout with this one exception. The 0.065 M solution gives rise to a depletion over a shorter length scale, 32 Å. While the ionic radius of TMA^+ (2.9 Å)[14] is larger than typical cations such as Na^+ (0.97 Å) K^+ (1.33 Å) or anions Br^- (1.96 Å) and Cl^- (1.81 Å)[15] in comparison the length scales of depletion are of longer range. Hence, we speculate that the depletion of ions near the substrate are not due to counterion size, or colloid effects, but due to electrostatics.

We can obtain some insight into this counterion depletion effect from an extension of Debye-Hückel theory to include a plane boundary of prescribed dielectric properties by Aqua and Cornu [16]. While this mean field theory naturally leads to a depletion length on the order of κ^{-1} (the basic length of Debye-Hückel theory,) rather than the polymer radius of gyration as in our experiments, it does address the qualitative effects of how the dielectric properties of the boundary influence the counterion distribution [17]. In particular, this mean field theory [16] of inhomogeneous ionic solutions predicts a counterion depletion near the solid substrate when the substrate dielectric constant, relative to the solution, is less than unity, while an enhancement of the counterion concentration can occur near the surface when this dielectric ratio is greater than unity. Moreover, in the case where this ratio should be less than unity as in the present experiments, the depletion layer thickness is predicted to decrease with an increased electrolyte or base concentration. These general trends are expected to be robust for our more complex charged fluids, although the actual size of the depletion layers should more naturally reflect the size of the molecules in fluids in which inter-particle interactions are larger. If these considerations are generally true, then the dielectric properties of the substrate should have a strong influence on the counterion distribution in these polyelectrolyte layers, playing a role comparable to the polymer-surface interaction in the density profiles of uncharged polymer layers [18]. It is interesting to note that this result can be tested using anti-reflective coatings (ARC), since the dielectric constant can be tuned by comparing organic versus inorganic ARCs.

3.3.Combined Polymer (Full Contrast) and Base Profiles (ZAC)

The polymer profile from the FC-NR experiment is compared to the ZAC-NR at the same base concentration (0.0325 M), providing complementary profiles as shown in Figure 5. The Q_C^2 difference beyond the solid / liquid interface arises from the SLD difference between the *d*-TMAH in ZAC solvent versus *h*-TMAH in D_2O. The polymer / liquid interface is determined by the intersection of the terminal thickness from the FC-NR experiment, shown as the dotted line. An excess of base is observed beyond the polymer total film thickness, overlapping the polymer profile at a base concentration of 0.0325 M. The counterion interfacial width of 29 Å results from two contributions; the counterion species that are closely associated with the chain, resembling a semidilute solution, and those that are unassociated, analogous to a surface excess at a charged interface. These chain segments will comprise the propagating dissolution front requiring a redistribution of counterion species during the course of dissolution. These initial stage dissolution

experiments highlight possibilities for tuning variables governing the interfacial structure of the dissolving polyelectrolyte layer.

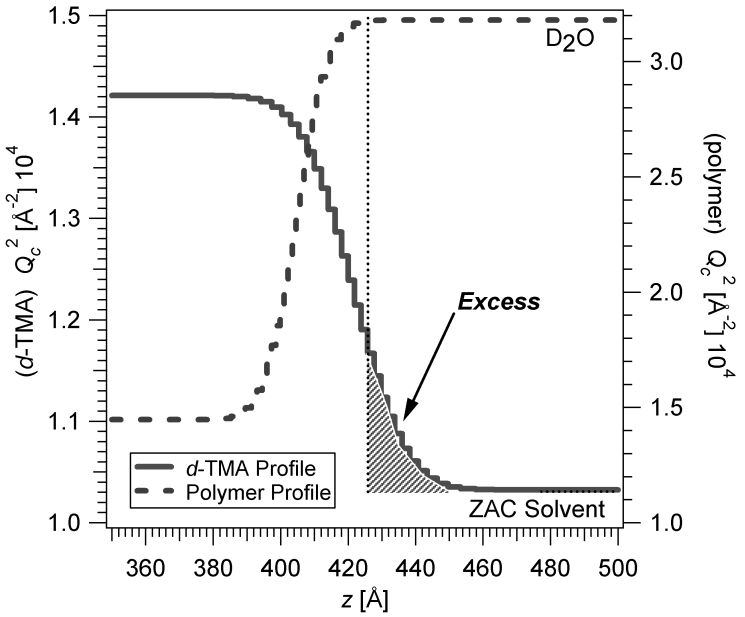

Figure 5. Excess *d*-TMA counterion at the periphery of the solid PNBHFA interface defined by a combination of zero-average and full contrast neutron reflectivity.

3.4.Dry Film State

A series of films exposed to *d*-TMAH in pure H_2O was examined to quantify the residual d-TMAH remaining within the film after swelling. The films were swollen for 25 min, then either immediately dried, or rinsed in pure H_2O for 30 s as shown in Figure 6a. The average volume fraction of *d*-TMAH was calculated from the measured $Q_C^2{}_{film}$ in a manner similar to Eq. 1. It is clear that the rinse step is crucial in removing residual trapped base. It is anticipated that swelling occurring at the line-edge would also lead to base penetration in the film due to a broad deprotection front[10,19]. In order to examine the effect of swelling extent on the surface roughness films were immersed in 0.065 M TMAH for a series of times ranging from (60 to 1000) s followed by a 60 s water rinse. The impact of swelling, without dissolution in the present case, does not lead to changes in surface roughness as characterized by the root-mean square (RMS) roughness from atomic force microscopy as shown in Figure 6b. Hence, without a dissolution-component, swelling alone does not impact the surface roughness in these homopolymer films.

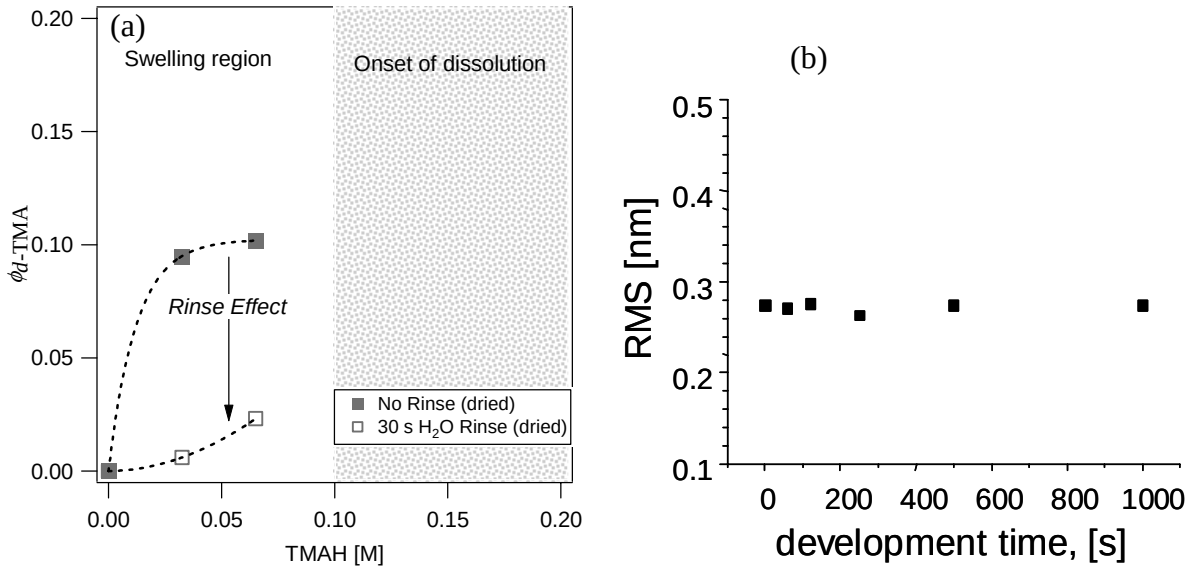

Figure 6. (a) Quantification of residual base trapped within ultrathin films. (b) Surface root-mean square (RMS) roughness of PNBHFA films immersed in 0.065 M developer as a function of time followed by a 60s water rinse.

4. CONCLUSIONS

Neutron reflectivity measures a non-uniform base developer counterion profile with depletion at the substrate and an accumulation at the polymer / solution interface. While a simple generalization of Debye-Hückel to include a boundary is unable to quantitatively describe the scale of the base depletion layer, it does indicate that the dielectric mismatch between the substrate boundary and the polyelectrolyte solution should be a relevant factor in determining the counterion distribution. The decrease in the relative size of the depletion layer with an increase of base or electrolyte concentration are qualitatively consistent with this high idealized model. We note that extensive hydrogen bonding reduces the accessibility of the acidic proton near the substrate which could be another factor influencing the counterion depletion effect. The solid film expansion depends linearly on the degree of ionization in these initial swelling stages of dissolution. A full understanding of the counterion distribution in thin films will require a better understanding of ionic polyelectrolyte solutions with boundary inhomogeneities.

ACKNOWLEDGEMENTS

We thank Bill Hinsberg and Frances Houle for many fruitful discussions and Michael Wang for assistance with the AFM measurements. This work was supported by the Defense Advanced Research Projects Agency under grant N66001-00-C-8083 and the NIST Office of Microelectronics Programs.

REFERENCES

1. W.D. Hinsberg, F.A. Houle, H. Ito, K. Kanazawa, and S.W. Lee, Proceedings of the 13th International Conference on Photopolymers, Advances in Imaging Materials and Processes, RETEC 2003 , 193 (2003).

2. Ueberreiter, K., *Diffusion in Polymers, The Solution Process*,(Academic Press, 1968) Chap. 7, pp.220-257.
3. W.D. Hinsberg, F.A. Houle, and H. Ito, Proceedings of the SPIE, Advances in Resist Technology and Processing XXI **5376**, 352 (2004).
4. F.A. Houle, W.D. Hinsberg, M. Morrison, M.I. Sanchez, G. Wallraff, C. Larson, and J. Hoffnagle, Journal of Vacuum Science & Technology B **18**(4), 1874 (2000).
5. F. Houle, W. Hinsberg, and M. Sanchez, Macromolecules **35**, 8591 (2003).
6. H. Ito, H.D. Truong, L.F. Rhodes, C. Chang, L.J. Langsdorf, H.A. Sidaway, K. Maeda, and S. Sumida, Journal of Photopolymer Science and Technology **17**(4), 609 (2004).
7. Y. Tran, P. Auroy, L.T. Lee, and M. Stamm, Physical Review E **60**(6), 6984 (1999).
8. F. Horkay and P.J. Basser, Biomacromolecules **5**(1), 232 (2004).
9. Flory,P.,*Principles of Polymer Chemistry, Phase Equilibria*,(Cornell University Press, Ithaca, 1953) Chap. XIII, p.577.
10. F.A. Houle, W.D. Hinsberg, and M.I. Sanchez, Macromolecules **35**(22), 8591 (2002).
11. L.W. Flanagin, C.L. McAdams, W.D. Hinsberg, I.C. Sanchez, and C.G. Willson, Macromolecules **32**(16), 5337 (1999).
12. M. Muthukumar, Journal of Chemical Physics **105**(12), 5183 (1996).
13. H. Ito, W.D. Hinsberg, L. Rhodes, and C. Chang, Proceedings of the SPIE, Advances in Resist Technology and Processing XX **5039**, 70 (2003).
14. J. Turner, A. Soper, and J. Finney, Molecular Physics **70**(4), 679 (1990).
15. *Handbook of chemistry and physics*, 54 ed. RC Weast (CRC Press, Cleveland, OH, 1974).
16. J.N. Aqua and F. Cornu, Journal of Statistical Physics **105**(1-2), 211 (2001).
17. The proper characteristic scale of is (κ^{-1} + *b*),hence the size (*b*) of the simple ion also dictates the range over which the inhomogeneous distribution heals in addition to the ionic strength.
18. M.S. Kent, Macromolecular Rapid Communications **21**(6), 243 (2000).
19. E.K. Lin, C.L. Soles, D.L. Goldfarb, B.C. Trinque, S.D. Burns, R.L. Jones, J.L. Lenhart, M. Angelopoulos, C.G. Willson, S.K. Satija, and W.L. Wu, Science **297**(5580), 372 (2002).